ACS Synthetic Biology

Article

Efflux pump control alters synthetic gene circuit function

Junchen Diao, Daniel Charlebois, Dmitry Nevozhay, Zoltan Bodi, Csaba Pal, and Gabor Balazsi

ACS Synth. Biol., **Just Accepted Manuscript** • DOI: 10.1021/acssynbio.5b00154 • Publication Date (Web): 25 Apr 2016

ACS Publications

ACS Synthetic Biology is published by the American Chemical Society. 1155 Sixteenth Street N.W., Washington, DC 20036

Efflux pump control alters synthetic gene circuit function

Authors: Junchen Diao[1], Daniel A. Charlebois[2], Dmitry Nevozhay[1,3], Zoltán Bódi[4], Csaba Pál[4], and Gábor Balázsi[1,2,5]*

Affiliations:

[1] Department of Systems Biology – Unit 950, 7435 Fannin Street, The University of Texas MD Anderson Cancer Center, Houston, TX 77054, USA

[2] The Louis and Beatrice Laufer Center for Physical & Quantitative Biology, 115C Laufer Center, Z-5252, Stony Brook University, Stony Brook, NY 11794, USA

[3]School of Biomedicine, Far Eastern Federal University, 8 Sukhanova Street, Vladivostok, 690950, Russia

[4] Institute of Biochemistry, Biological Research Centre of the Hungarian Academy of Sciences, Temesvári krt. 62., H-6726 Szeged, Hungary

[5] Department of Biomedical Engineering, Z-5281, Stony Brook University, Stony Brook, NY 11794, USA

*To whom correspondence should be addressed:

Tel: 631-632-5414
Fax: 631-632-5405
Email: gabor.balazsi@stonybrook.edu

Abstract

Synthetic biology aims to design new biological systems for predefined purposes, such as the controlled secretion of biofuels, pharmaceuticals, or other chemicals. Synthetic gene circuits regulating an efflux pump from the ATP-binding cassette (ABC) protein family could achieve this. However, ABC efflux pumps can also drive out intracellular inducer molecules that control the gene circuits. This will introduce an implicit feedback that could alter gene circuit function in ways that are poorly understood. Here, we used two synthetic gene circuits inducible by tetracycline family molecules to regulate the expression of a yeast ABC pump (Pdr5p) that pumps out the inducer. Pdr5p altered the dose-responses of the original gene circuits substantially in *Saccharomyces cerevisiae*. While one aspect of the change could be attributed to the efflux pumping function of Pdr5p, another aspect remained unexplained. Quantitative modeling indicated that reduced regulator gene expression in addition to efflux pump function could fully explain the altered dose-responses. These predictions were validated experimentally. Overall, we highlight how efflux pumps can alter gene circuit dynamics and demonstrate the utility of mathematical modeling in understanding synthetic gene circuit function in new circumstances.

Keywords: synthetic gene circuit, efflux pump, stochastic simulation, feedback

Synthetic biology aims to build biological devices for predefined purposes[1-5]. One important goal for synthetic biologists is to construct synthetic gene circuits[6, 7] that function as switches, oscillators, logic gates, dimmers, or counters[8-16]. Small molecule inducers that bind to the protein components of such gene circuits are often used to control them externally. The hope is that by placing specific genes under the control of such inducible synthetic gene circuits, users can deliver precise stimuli to cell populations[17-20]. For example, synthetic gene circuits could enable the controlled secretion of drugs or biofuel compounds for clinical or industrial purposes[21, 22]. Secreting drugs and biofuels requires efflux pumps that actively move them across the cell membrane. ATP-binding cassette (ABC) family multidrug resistance pumps are prime candidates to fulfill this function. Highly conserved across bacteria, fungi, and mammals, ABC family efflux pump proteins cause microbial resistance to antibiotic treatment and chemoresistance in tumors by pumping out a wide range of compounds into the extracellular medium[23]. Importantly, in addition to their intended substrates, efflux pumps can also drive out the intracellular inducer and thereby reduce its concentration. This creates a feedback loop[24] that may alter the function of synthetic or natural gene networks that control efflux pump protein expression. Understanding the effect of this implicit feedback is important if efflux pumps are to be used as parts of synthetic gene circuits. Yet, the effect of efflux pumps on synthetic gene circuit function has not been thoroughly investigated.

Our goal here was to study the interaction between an efflux pump and two synthetic gene circuits that regulate it. To achieve this, we modified two TetR-based synthetic gene circuits, called “Negative Regulation” (NR) and “Negative Feedback” (NF), both inducible by tetracycline analogs. We have previously characterized versions of these gene circuits that

controlled a passive target gene (yEGFP::zeoR), which does not affect its upstream transcriptional regulator. Here, we replaced this passive target gene with the yeast pleiotropic drug resistance (PDR) pump-fluorescent reporter fusion gene *PDR5::GFP*. Once the Pdr5p::GFP protein is expressed, it pumps out the inducer[25-27], altering the activity of its transcriptional regulator, and thereby creating a feedback loop. We studied by experiment and mathematical modeling whether this implicit feedback loop altered the dose-response of the original gene circuits as intuitively expected from efflux pump function. Surprisingly, we observed an additional and unexpected dose-response change after introducing the gene that encoded the efflux pump. Using a combined mathematical-experimental approach, we identified reduced TetR expression as the cause underlying this additional change. These findings shed light on how efflux pumps can alter gene network function and highlight the importance of mathematical modeling in elucidating unexpected consequences of gene circuit modifications.

RESULTS AND DISCUSSION

Efflux pump alters the dose-response of the NR synthetic gene circuit

To understand how an efflux pump affects the function of its transcriptional regulatory network, we modified the previously characterized [16] "negative regulation" (NR) gene circuit to create a new gene circuit, NRpump. Both NR and NRpump consisted of two parts: a *target gene* and a *regulator gene* (**Figure 1A**,**B**). The regulator gene in both gene circuits was the *tetR* repressor under the control of the natural *PGAL1* promoter [16], which is constitutively active in galactose-containing media. The TetR protein can repress gene transcription by binding to *tetO2* operator sites in the target promoter. In the NR gene circuit, the target gene was *yEGFP::zeoR* (*yEGFP* fused to *zeoR*) under the control of *GAL1-D12*, a *GAL1* promoter modified to contain two *tetO2* operator sites[28] (**Figure 1A**). In the NRpump gene circuit, the target gene was *PDR5::GFP* (**Figure 1B**), which can remove the inducer doxycycline from the cell interior [29-31]. To avoid potential confounding interference with the native copy of *PDR5*, both gene circuits were chromosomally integrated into endogenous *PDR5*-knockout yeast cells (**Figure S1**). Overall, the NR and NRpump gene circuits differed only in their target gene: NR contained the passive target gene *yEGFP::zeoR*[16], whereas NRpump contained the active target gene *PDR5::GFP*. Throughout the paper, the term "pump" will indicate the inclusion of *PDR5* into gene circuits and the implicit feedback generated through inducer removal.

To determine how the efflux pump alters NR gene circuit function, we measured experimentally (by flow cytometry) the dose-responses of fluorescence intensity in both NR and NRpump with respect to the same inducer, doxycycline (**Figures 1C-F**). Flow cytometry is a

quantitative, highly reproducible method for measuring protein levels in yeast[32], producing results consistent with those of other measurement techniques, including Western Blotting[32, 33]. Plotting mean reporter (yEGFP::ZeoR or Pdr5p::GFP) fluorescence intensity at increasing doxycycline concentrations (**Figure 1E**) revealed a sigmoidal dose-response of mean target gene expression in both gene circuits, with a steep increase at intermediate inducer concentrations. However, compared to NR, the reporter in NRpump began to express at lower doxycycline concentrations. Phrased differently, NRpump was more inducer-sensitive at low induction. The opposite was true at high doxycycline concentrations: the NRpump gene circuit required higher doxycycline concentrations to reach saturation, meaning that it was less inducer-sensitive at high induction.

The experimentally measured gene expression noise, characterized by the coefficients of variation (CVs) (standard deviation normalized by the mean), peaked at a slightly lower doxycycline concentration and reached a lower maximum for NRpump compared to NR (**Figure 1F**). The CV peaks (**Figure 1F**) corresponded to the broad histograms at intermediate doxycycline concentrations (**Figures 1C** and **1D**), indicating heterogeneous reporter expression in the cell population. The lower CV peak for NRpump could be due to pump-mediated negative feedback, which is known to reduce noise [34-36].

In summary, we observed two dose-response changes in NRpump compared to NR: increased inducer-sensitivity at low induction and decreased inducer-sensitivity at high induction. The latter observation (decreased inducer-sensitivity in high doxycycline) could be intuitively explained by the Pdr5p::GFP pump removing some doxycycline molecules from the cell interior, thereby lowering inducer-sensitivity. On the other hand, the increased inducer sensitivity at low inducer concentrations was counterintuitive.

A mathematical model of the pump-mediated dose-response change

To better understand the dose-response changes in the NRpump gene circuit relative to NR, we turned to computational modeling. We previously established a computational model to simulate the NR dose-response[16]. Here, we verified that stochastic simulations based on this earlier model were able to reproduce our experimental NR dose-response observations (**Figure 2A,B** and **Figure S2**). Then we introduced, using Michaelis-Menten kinetics, an efflux pump term into this earlier model to simulate the changes in the NRpump dose-response relative to NR (see the Methods). However, the modified model could only partially reproduce the dose-response change in the NRpump gene circuit relative to NR (**Figure 2A**,**B**). Specifically, the addition of the pump term reproduced decreased inducer-sensitivity at high doxycycline concentrations, in agreement with experimental results. However, it failed to reproduce the increased inducer-sensitivity at low doxycycline concentrations.

To restore agreement with the experimental data, we analyzed the parameter sensitivity of the model (**Table S1**). This analysis revealed that both aspects of the dose-response change in NRpump could be reproduced only if the repressor protein (TetR) production rate was reduced in addition to introducing the pump term. Similar effects from altered regulator expression have been observed before[37]. A new model that included this effect successfully reproduced both increased inducer-sensitivity at low inducer concentrations and decreased inducer-sensitivity at high concentrations, as in the experimental NRpump dose-response data (**Figures 2C**,**D**).

Efflux pump alters the dose-response of the NF synthetic gene circuit

To test the predictive power of the computational model, we set out to also predict the pump-mediated dose-response change for a related gene circuit[16], called "Negative Feedback" (NF) or "linearizer". The NF gene circuit is similar to NR, except for the promoter driving *tetR* expression, which is replaced with the TetR-repressible promoter that also controls target gene expression (**Figure 3A**). Therefore, NF incorporates negative feedback compared to NR, because TetR represses its own expression (in addition to the target gene). Remarkably, the mean NF dose-response for yeast [16] and mammalian[19] cells carrying the NF gene circuit was linear nearly up to saturation.

To predict how efflux pump protein regulation may affect the dose-response of the NF gene circuit, we first introduced TetR negative feedback into the NR mathematical model as previously[16], and confirmed that the dose-response became linear before saturation. Then we introduced the same pump term as in the NRpump model, and found that the simulated NFpump dose-response became concave, curving downward while staying always below the NF dose-response curve (**Figure S3**). Finally, to predict the additional effect(s) of reducing TetR synthesis on the NFpump gene circuit's dose-response, we changed the same parameter as in the NRpump model to reduce TetR synthesis rate. The numerical solutions of the latter NFpump model predicted a dose-response that was still concave, but was above the NF dose-response, indicating increased inducer-sensitivity for NFpump (**Figure 3C**). On the other hand, the simulated CVs of both NF and NFpump were similarly low at all inducer levels (**Figure 3D**).

To test these computational predictions experimentally, we constructed the NFpump gene circuit in a manner similar to NRpump. Then we measured by flow cytometry the dose-responses

of fluorescence intensity for the NF and NFpump gene circuits at increasing concentrations of doxycycline (**Figure 3E-H**). The results confirmed that NF had a linear fluorescence mean dose-response between doxycycline concentrations 0 μg/ml and 4 μg/ml. By contrast, the mean dose-response for NFpump was concave (not linear) (**Figure 3E**), and lay above the NF dose-response (**Figure 3E**), as predicted computationally when TetR synthesis rate was reduced in addition to introducing the pump term (**Figure 2C**). Gene expression noise for both NF and NFpump was low at all levels of induction (**Figure 3F**). Accordingly, the fluorescence histograms of both NF and NFpump were narrow and uniform at all doxycycline concentrations (**Figure 3G** and **3H**).

In summary, introducing the efflux pump altered two aspects of the NF gene circuit's mean dose-response, causing loss of dose-response linearity and increased inducer-sensitivity. This agreed with computational models that had reduced TetR synthesis besides including the efflux pump term.

Efflux pump mutants reveal that pump function is insufficient to explain dose-response differences

Our findings so far indicated that the shapes of the mean dose-response curves in both NRpump and NFpump changed in two different ways compared to NR and NF, respectively. Computational simulations predicted that the most likely causes of these changes were the efflux pumping function of Pdr5p combined with lower TetR expression. Therefore, we set out to test experimentally if Pdr5p efflux pump function alone was indeed insufficient to produce both aspects of NRpump and NFpump mean dose-response change.

To test the effect of efflux pump function on the dose-response separately from any other effects, we constructed two Pdr5p functional mutants, Pdr5p-S558Y and Pdr5p-G312A. Both mutants should disrupt the association between Pdr5p and ATP, thereby significantly compromising the efflux pumping function of Pdr5p[25, 26]. Thus, we replaced the wild-type *PDR5* gene with each of these mutant genes in the NRpump and NFpump gene circuits and integrated the new gene circuits separately into the parental yeast genome to create two new "NRpumpmutant" and "NFpumpmutant" strains: NRpump-558, NRpump-312, NFpump-558 and NFpump-312.

Next, we measured experimentally the mean dose-responses and CV dose-responses of NRpump-312 and NRpump-558, and compared them with NR and NRpump. The experimental results showed that NRpumpmutant strains responded to doxycycline concentrations as low as 4 μg/ml (**Figure 4A-C** and **Figure S4A**). This resembled the increased inducer-sensitivity of NRpump (**Figure 1E**). On the other hand, the mean dose-response curves of NRpumpmutant strains increased as steeply as for NR at intermediate induction (4 μg/ml to 6 μg/ml doxycycline), contrasting the gradual dose-response of NRpump (**Figure 4C**). The dose-responses of CVs were similar for all strains, except that the CV of NR peaked at slightly higher doxycycline concentration than the other three strains (**Figure 4D**), according to the decreased inducer-sensitivity of NR. These experiments confirmed that the efflux pumping function of Pdr5p caused the dose-response change at high doxycycline concentrations, but not at low doxycycline concentrations.

Afterwards, we measured the experimental dose-responses of the reporter means and CVs of NFpumpmutant strains. Both NFpumpmutant strains had linear dose-responses between doxycycline concentrations 0 and 2 μg/ml similar to NF, and saturated at 3 μg/ml (**Figure 5A-C**

and **Figure S4B**). Recovering linearity in the NFpumpmutant strains indicated that the dose-response concavity in NFpump was most likely due to the efflux pumping function of Pdr5p::GFP. However, the slopes of the linear ranges in both NFpumpmutant strains were still higher than that in NF. This suggested that the non-functional pump gene somehow still increased the sensitivity of the NFpumpmutant gene circuits to doxycycline concentration, similar to NFpump.

Accordingly, as we lowered efflux pumping rate in NRpump and NFpump computational models with reduced TetR synthesis, we obtained dose-responses similar to the experimentally observed NRpumpmutant and NFpumpmutant dose-response curves (**Figure 6A** and **6C**), which still differed from those of NR and NF.

Both the experimentally measured and simulated CVs for NFpumpmutant strains were similarly low and slightly decreasing as the NF and NFpump gene circuits, consistent with the narrow and uniform distribution of reporter expression observed by single cell-level measurements (**Figures 5D** and **6D**). Likewise, the doxycycline concentration at which the CV peaks occurred in the NR, NRpump, and NRpumpmutant strains, as well as the relative size of the peaks, were consistent between computational models and experimental observations (**Figures 4D** and **6B**).

Overall, we found that there was still a difference between the mean fluorescence dose-responses of NRpumpmutant and NR as well as NFpumpmutant and NF strains, whether or not the pump was functional (**Figure S4** shows mean dose-responses without normalization). Thus, we confirmed the computational predictions that the efflux pumping function of Pdr5p is insufficient to fully explain the dose-response change. Specifically, it cannot cause the increased

inducer-sensitivity observed in NRpump and NFpump (although it most likely causes the decreased inducer-sensitivity of NR high doxycycline and concavity of NFpump dose-response).

Experimental confirmation of lower TetR expression in NRpump and NFpump strains.

So far we have shown that efflux pump activity of Pdr5p only explains one aspect of the dose-response changes in NRpump and NFpump. Computational models suggested lower TetR expression causing the other aspect (increased inducer-sensitivity). To confirm whether regulator gene expression was indeed lower in all other strains compared to NR and NF, as predicted computationally, we fused TetR with the fluorescent reporter, mCherry, and then replaced the original TetR with this bifunctional fusion in all of the 8 synthetic gene circuits mentioned above. Thus, by combining *tetR::mCherry* with *yEGFP::zeoR* for NR and NF, and *tetR::mCherry* with *PDR5::GFP* for all other strains, including the efflux pump mutants, we created eight 2-color (2c) gene circuits (**Figure 7**). Importantly, all of the experiments described above could have been done with these two-color gene circuits. Therefore, if the dose-response changes in the 2-color strains are consistent with those in the corresponding single-color strains, then the 2-color strains are appropriate means to investigate the causes of any dose-response changes in single-colored strains.

We induced all the 2-color strains with the same doxycycline concentrations as for the corresponding single-color counterparts. The dose-response changes of fluorescence means for the target gene in all 2-color strains were consistent with those of the corresponding single-color strains (compare, for example **Figures 8A** and **8B** with **3E**, and see **Figure S5**). Moreover, the

TetR::mCherry regulator expression's dose-responses in ^{2c}NF, ^{2c}NFpump and ^{2c}NFpumpmutant strains were also consistent with the reporter expression in the same strain and the corresponding single-color strains (**Figures 8A** and **8B**). On the other hand, TetR::mCherry expression level at all doxycycline concentrations remained the same in the ^{2c}NR, ^{2c}NRpump and ^{2c}NRpumpmutant strains (**Figure 8E**), as expected because the wild-type *GAL1* promoter driving *tetR::mCherry* expression in these strains is constitutively active in galactose-containing media, and should not respond to doxycycline. Thus, the 2-color strains are suitable to reveal all the causes of dose-response changes in single-colored strains.

To test if regulator expression levels were altered by introducing the efflux pump-encoding target gene, we measured the red fluorescence intensity of the regulator in all of the 2-color strains. Interestingly, by investigating TetR::mCherry expression levels in this way, we observed clone-dependent variation (**Figures 8C**,**D**), causing large error bars in **Figures 8E** and **8F**. In addition, there were some minor strain-dependent differences in TetR levels (**Figures 8C** and **8D**). Nevertheless, TetR::mCherry expression was always higher in NR and NF clones than in clones carrying any of the other gene circuits (**Figures 8C**,**D**), confirming our computational predictions. Furthermore, TetR::mCherry mean dose-response measurements indicated that the repressor had higher expression level in NR compared to NRpump and NRpumpmutant strains at all doxycycline doses (**Figure 8E**), as expected. In a similar agreement with computational predictions, TetR::mCherry expression level in NF was higher than that in NFpump and NFpumpmutant strains at all doxycycline doses (**Figure 8F**).

Overall, these experimental results from 2-colored strains confirmed the computational prediction that reduced regulator expression, rather than the efflux pumping function of Pdr5p, caused the unexpected aspect of dose-response changes (increased inducer-sensitivity). Thus,

both effects together (efflux pump function and reduced TetR expression) fully explain all of the observed the dose-response changes.

Discussion and outlook

We studied the effect of introducing an efflux pump into the previously characterized[16], tetracycline analog-inducible Negative Regulation (NR) and Negative Feedback (NF) synthetic gene circuits in *Saccharomyces cerevisiae*. We found that introducing *PDR5::GFP*, a multidrug resistance pump-reporter gene fusion, changed the dose-responses of the two gene circuits in both intuitively expected and unexpected ways. Namely, we intuitively expected that both NRpump and NFpump should be less inducer-sensitive than their non-pump counterparts, considering that Pdr5p can exclude tetracycline family molecules from the cell and thereby decrease intracellular inducer concentration[25-27]. This was indeed true at high induction – but not in general. These surprising results implied the existence of additional causes that modulate the dose-responses of NRpump and NFpump in unexpected ways. To uncover the causes of the unexpected effects, we turned to computational modeling. Interestingly, when we reduced the regulator synthesis rate, our simulations fully reproduced the dose-response changes we observed experimentally (**Figures 2C** and **3C**).

Therefore, we identified two potential causes that jointly resulted in the NRpump and NFpump dose-response changes: efflux pump function and regulator level reduction. To determine the effect of efflux pump function, we created NRpumpmutant and NFpumpmutant strains bearing *PDR5* mutants with compromised efflux pump function. The dose-responses of NRpumpmutant and NFpumpmutant strains only captured one aspect of each dose-response

change, indicating the insufficiency of pump function to fully explain the observations. Thus, to confirm the computationally predicted role of altered TetR levels, we measured regulator expression in all the strains by fusing mCherry to TetR. The experimental measurements confirmed that TetR had lower expression level in all other strains (whether or not Pdr5p was functional) compared to NR and NF strains, in agreement with computational predictions. Lower TetR level in these strains weakened the repression of *PDR5* transcription, causing increased inducer sensitivity, in agreement with previous observations[37].

The mechanism reducing TetR protein expression (**Figure 8**) is still unclear and needs further investigation. Pdr5p protein levels did not affect regulator expression since TetR::mCherry level remained the same, although Pdr5p protein levels increased with doxycycline in ^{2c}NRpump strains (**Figure 8**). Likewise, fluorescence measurements in NRpumpmutant and NFpumpmutant strains demonstrated that Pdr5p efflux activity did not reduce TetR levels. One possibility is that the integration of the *PDR5* gene upstream of *tetR*'s promoter impaired *tetR* transcription. This may have occurred only in *PDR5*-containing strains because the *PDR5* gene is over 5 kb long while the *zeoR* gene (in NR and NF) is only ~1 kb long. Another possibility is that epigenetic modifications (for example, methylation) of *PDR5* affects general transcription factor binding to *tetR*'s promoter. Finally, growth rate differences between NR and NRpump as well as NF and NFpump strains may have also altered TetR concentrations[38-42] (**Figure S6**).

To our knowledge, how an efflux pump alters the behavior of its synthetic or natural regulatory network has not been characterized experimentally or mathematically in a eukaryote. A related study used mathematical models to simulate the dynamics of natural interlinked negative and positive feedback loops that control an efflux pump in *E. coli*. Therefore, our

findings and methods may be useful for predicting and understanding expected and unexpected consequences of modifying natural and synthetic gene networks that regulate an efflux pump and/or other active target genes. In general, we expect that our methods will facilitate quantitative understanding of how the dose-responses and dynamics of efflux pump-regulating gene circuits will change. For example, genetic toggle switches might require higher inducer concentration to flip when they are controlling an efflux pump. Efflux pumps may also alter genetic oscillator dynamics, by creating secondary feedback on top of the primary delayed feedback needed to generate oscillations[14]. On the other hand, introducing *PDR5* into bistable networks with positive autoregulation may result in a new way to build oscillators.

Our findings suggest that the presence of multidrug resistance pumps in natural or synthetic gene networks can have predictable and unexpected consequences. First, pump terms similar to the ones we used should be generally applicable to model the effect of inducer removal from the cellular interior. In many cases, adding such terms to existing gene network models should be sufficient to predict their altered behavior. However, as the yeast gene circuits indicate, pump-encoding genes can have additional effects that are not predictable in advance. Nonetheless, even in these cases, mathematical modeling should help identify the causes of such additional changes. The methodology should be analogous to what we used above: first, test if including a pump term is sufficient to capture the altered behavior. If not, then perform a parameter scan to identify where the additional changes originate.

Besides new insight into altered gene circuit behavior, this study has numerous applications. The ability to precisely control Pdr5p expression using synthetic gene circuits with low noise (such as NF) may allow novel applications and quantitative studies of biological processes that involve efflux pumps. For example, recent work has shown that an efflux pump increased biofuel

production in *Escherichia coli* by exporting biofuel molecules outside of the bacteria and reducing their toxicity[21]. Also, negative feedback regulation of an efflux pump was found to increase the tolerance to a certain biofuel molecule, thereby improving its production rate [44]. Similarly, NFpump can regulate the secretion of intracellular biofuel molecules precisely, maintaining optimal balance between cellular fitness and productivity. Furthermore, combining synthetic gene circuits with biosensors could help cells detect certain molecules and respond automatically. For example, a recently engineered biosensor in yeast cells is able to detect steroid hormones[27]. An automatic system for production of steroids could be built by adding a biosensor to synthetic gene circuits with pumps to introduce feedback into hormone systems. Different concentrations of intracellular steroids will automatically result in different PDR5 expression to maintain hormone production at the desired level.

In addition to regulating biomaterial production, *PDR5*-containing gene circuits can also be used to advance basic research. A group of Pdr proteins in *Saccharomyces cerevisiae* has been shown to affect aging[45]. The NFpump gene circuit can tune the expression of such genes to study the aging process more precisely. Our system can also facilitate research on pump-mediated multidrug resistance (MDR). Earlier studies showed that transcriptional noise aided survival in stressful environments/conditions[46-50]. Thus, one cause for drug resistance could be MDR gene expression noise. Since the NF gene circuit reduces transcriptional noise, using NFpump and NRpump to independently control MDR pump levels and variability enables studying how cells survive drug treatment, how drug resistance evolves, and possibly, how to prevent it.

METHODS

Synthetic gene circuit construction:

Each synthetic gene circuit we used consisted of two parts originating from separate plasmids: the target gene (a bifunctional reporter-efflux pump fusion) and the regulator gene (**Figure 1**). We obtained the *PDR5::GFP* gene fusion (the target gene) by PCR amplification from whole-genome extraction of the GFP-tagged yeast library [51] and cloned it into the pRS4D1 integrative yeast plasmid, which was used to build the NRpump and NFpump gene circuits [46, 49], and chromosomally integrated into the *GAL1-GAL10* locus as previously described [16, 52]. In each NRpump558/312 and NFpump558/312 version, a single nucleotide mutation was introduced into the *PDR5* gene sequence before following the same procedure for yeast integration. In the S558Y mutant, the C was changed to A at nucleotide position 1673 in the *PDR5* gene. In the G312A mutant, the G was changed to C at nucleotide position 935 in the *PDR5* gene.

Strains and medium

The haploid *S. cerevisiae* strain YPH500 (α, *ura3-52*, *lys2-801*, *ade2-101*, *trp1*Δ*63*, *his3*Δ*200*, and *leu2*Δ*1*) (Stratagene) was used as a parental strain. The reporter plasmid was integrated into the native *GAL1-GAL10* locus first. Then the regulator plasmid was integrated into the *ampR* gene in the reporter plasmid by homologous recombination. The transformation procedure was described previously [53]. Strains with single integration were selected by PCR and flow cytometry. All cell cultures were grown in synthetic drop-out (SD) medium with appropriate selection markers and 2% galactose.

Reporter gene expression and measurement

Strains were streaked on agar plates with SD medium and 2% glucose, and grown at 30°C for 2 days. Single colonies were selected from the plates and incubated overnight in liquid SD medium supplemented with 2% galactose and appropriate selection markers at 30°C. Then the cell cultures were suspended into fresh SD medium of the same composition with starting cell density of $5x10^5$ cells/ml (determined using a NexCelom Cellometer Auto M4). Cells were resuspended regularly every 12 hours with the same starting cell density into fresh medium of the same composition over the entire length of the experiment. In dose-response experiments, cells were suspended in SD medium with 2% galactose, appropriate selection markers and increasing doxycycline concentrations, which varied from strain to strain. Flow cytometry was used to measure reporter gene expression every 24 hours after reporter gene expression became stable (the fluorescence intensity histogram did not change from one day to the next). A gate based on Forward Scatter (FSC) and Side Scatter (SSC) was used to filter out non-living cells, doublets and cell debris.

Data analysis

Flow cytometry data was processed in Matlab by the Mathworks, Inc. FSC, SSC and fluorescence intensity for all living cells were extracted and used to assign gates to select the most concentrated cell population in each sample to exclude external noise, such as difference in cell size and shape. Then fluorescence intensity for gated cells was extracted and read within the specified gate. Cells with log fluorescence deviating >3 standard deviations from the arithmetic mean were considered outliers and were discarded from the analysis (based on our experience, these were rare cells left over from previous samples). Arithmetic mean and coefficient of

variation (CV), defined as the standard deviation divided by the mean of fluorescence intensity, were calculated for gated cells for each sample. Mean and CV was then plotted for each dose-response assay.

Computational modeling and data fitting

On the basis of the previously published mathematical model [16], we established differential equations to simulate the dose-response of cells with an NR gene circuit regulating a pump as follows:

$$\frac{dx}{dt} = a_x F_x(x) - bxy - dx$$

$$\frac{dy}{dt} = C - bxy - fy - \frac{ky^h z}{(K^h + y^h)}$$

$$\frac{dz}{dt} = l_z + a_z F_z(x) - dz$$

Here the variables x, y, and z correspond to free intracellular repressor (TetR), inducer (doxycycline), and pump/reporter (Pdr5p::GFP) protein concentrations, respectively. C is a control parameter proportional to extracellular inducer concentration. Repressor protein synthesis rate is a_x, pump/reporter protein synthesis rate is a_z, leaky pump/reporter protein synthesis rate is l_z, inducer–repressor association rate is b, the rate of dilution due to cell growth is d, the combined rate of inducer dilution and degradation is f, the inducer concentration at which pump

activation is half-maximal is *K,* the pump Hill coefficient is *h*, and rate of Pdr5p mediated inducer efflux is *k* (*k* = 0 for the NR circuit, and *k* > 0 for the NRpump circuit).

The functions $F_x(x)$ *and* $F_z(x)$ are Hill functions that respectively describe the repressor dependence of protein synthesis from the upstream and downstream promoters:

$$F_x(x) = F_z(x) = \frac{\theta^n}{\theta^n + x^n}$$

Here, θ is the induction threshold and *n* the corresponding Hill coefficient (F_x = 1 for NR and NRpump circuits, and $F_x = F_z$ for NF and NFpump circuits).

These parameters were obtained by fitting the model to experimental data. An analytic solution for *z* as a function of the control parameter *C* is available for the NR circuit case (see ref. [28] for details):

$$z(C) = \frac{l_z + a_z F_z(x(C))}{d}$$

where

$$x(C) = \frac{(a_x b - df - bC) + \sqrt{(a_x b - df - bC)^2 + 4bda_x f}}{2bd}$$

The analytic equation was fit to the experimental data for the NR strain using Matlab's curve fitting application (fit options: Nonlinear Least Squares, algorithm: Trust-Region, $r^2 = 0.9991$) guided by biologically realistic parameter lower and upper bounds (**Figure S2**). Fitting for the other strains was based on these parameters, tuning additional parameters by hand to fit the

experimental data. Computational results for the ODE model were obtained using Malab's ode45 differential equation solver and were used together with experimental data to guide stochastic simulations.

The system of ordinary differential equations was converted to the following reaction equations and simulated using the Gillespie stochastic simulation algorithm [54, 55]:

$$\varnothing \xrightarrow{\kappa_x} x$$

$$x \xrightarrow{\delta_x} \varnothing$$

$$\varnothing \xrightarrow{\kappa_y} y$$

$$y \xrightarrow{\delta_y} \varnothing$$

$$x + y \xrightarrow{\lambda} \varnothing$$

$$\varnothing \xrightarrow{\kappa_z} z$$

$$z \xrightarrow{\delta_z} \varnothing$$

where $\kappa_x = a_x F_x$, $\delta_x = d$, $\kappa_y = C$, $\delta_y = f + ky^{-1}(y^h/K^h + y^h)z$, $\lambda = b$, $\kappa_z = l_z + a_z F_z$, and $\delta_z = d$. All simulation results were obtained from 20 realizations of 1000 cells.

FUNDING

This research was supported by the NIH Director's New Innovator Award Program (1DP2 OD006481-01) and by the Laufer Center for Physical & Quantitative Biology to GB; by the Lendület Program of the Hungarian Academy of Sciences, The Wellcome Trust International Senior Research Fellowship (WT084314MA) and the European Research Council (ERC-2007-StG) to CP; by the University of Texas Graduate School of Biomedical Sciences at Houston to JD; Program # 1326 of the Ministry of Education and Science, Russian Federation to DN and by a Natural Sciences and Engineering Research Council of Canada Postdoctoral Fellowship [Grant no: PDF-453977-2014] to DC.

Conflict of interest statement. None declared.

ACKNOWLEDGEMENTS

We thank W.-K. Huh for kindly sharing the PDR5::GFP fusion, and M. Bennett, M. Lorenz, G. May, T. F. Cooper and G. Peng for helpful discussions.

Author Contributions

JD, DC, CP and GB designed research; JD, DN, and ZB performed experiments; JD analyzed the data; DC developed mathematical models and performed simulations; and JD, DC and GB wrote the paper.

Figure captions

Figure 1. Experimentally measured dose-responses of the NR and NRpump strains. (A) Negative Regulation (NR) gene circuit design. This gene circuit consists of a regulator gene (*tetR*) that represses target gene (*yEGFP::zeoR*) expression in a doxycycline concentration-dependent manner. Red blunt arrows indicate repression. **(B)** Negative Regulation pump (NRpump) gene circuit design. This gene circuit is identical to NR, except for the target gene (*PDR5::GFP* in this case). Note that the Pdr5p efflux pump transports doxycycline out of the cell, creating an implicit feedback loop (blue blunt arrow) in NRpump, which does not exist in NR. **(C)** Experimentally measured histograms of fluorescence intensity for the NR gene circuit, indicating yEGFP::zeoR expression at increasing doxycycline concentrations. **(D)** Experimentally measured histograms of fluorescence intensity for the NRpump gene circuit, indicating PDR5::GFP expression at increasing doxycycline concentrations. **(E)** Experimentally measured dose-responses of NR (black) and NRpump (red) mean fluorescence intensity. These and all subsequent mean dose-responses were normalized by the maximum fluorescence intensity such that normalized fluorescence values fall between 0 and 1. **(F)** Experimentally measured dose-responses of NR (black) and NRpump (red) Coefficients of Variation (CVs).

Figure 2. Stochastic simulation of pump-mediated dose-response change. (A) Stochastic simulation of NR (black) and NRpump (red) mean dose-responses. The simulations for NR are based on previous models[16], with only an efflux pump term added for NRpump. **(B)** Stochastic simulation of NR (black) and NRpump (red) CV dose-responses, with only an efflux pump term added to previous models, as described above. **(C)** Stochastic simulation of NR (black) and NRpump (red) mean dose-responses with an efflux pump term added and TetR synthesis rate reduced compared to previous models. **(D)** Stochastic simulations of NR and NRpump CVs with an efflux pump term added and TetR synthesis rate reduced compared to earlier models. Most parameters in (A) and (B) were based on a previous model[16] (except for l_z, K, h, and k, which were obtained by fitting the data) as follows: $a_x = a_z = 50$ nM h^{-1}, $l_z = 10$ nM h^{-1}, $b =$ 10 nM^{-1}, $C = 10$ [dox] h^{-1}, $d_x = d_z = 0.12$ h^{-1}, $d_y = 1.2$ h^{-1}, $\theta = 0.44$ nM, $n = 4$, $K = 50$ nM, $h = 3.5$, and $k =$

0 h^{-1} for NR strain. All parameters were identical for the NRpump strain, except enabling pump function by setting k = 200 h^{-1}. The same parameters were used in (C) and (D) as in (A) and (B), respectively, except for lowering a_x = 43 nM h^{-1} for the NRpump strain.

Figure 3. Computationally predicted and experimentally measured dose-responses of the NF and NFpump strains. (A) NF gene circuit design. This gene circuit differs from NR in a single aspect: TetR autorepression (negative feedback). **(B)** NFpump gene circuit design. This gene circuit differs from NRpump in a single aspect: TetR autorepression (negative feedback). It differs from NR in two aspects, each creating a feedback loop: TetR autorepression and an implicit feedback through Pdr5p::GFP pump function. **(C)** Stochastic simulation of NF (black) and NFpump (red) mean dose-responses with an efflux pump term added and TetR synthesis rate reduced compared to previous models[16]. **(D)** Stochastic simulation of NF (black) and NFpump (red) CV dose-responses with an efflux pump term added and TetR synthesis rate reduced compared to previous models. **(E)** Experimentally measured NF (black) and NFpump (red) mean dose-responses. **(F)** NF and NFpump CV dose-responses (experimental data). **(G)** Experimentally measured histograms of fluorescence intensity for the NF gene circuit, indicating yEGFP::zeoR expression at increasing doxycycline concentrations. **(H)** Experimentally measured histograms of fluorescence intensity for the NFpump gene circuit, indicating PDR5::GFP expression at increasing doxycycline concentrations. Parameters for the stochastic simulations were the same as described in the legend of Figure 2, and were set to: $a_x = a_z$ = 50 nM h^{-1}, l_z = 10 nM h^{-1}, b = 10 nM^{-1}, C = 10 [dox] h^{-1}, $d_x = d_z$ = 0.12 h^{-1}, d_y = 1.2 h^{-1}, K = 50 nM, h = 3.5, θ = 0.44 nM, n = 4, k = 0 h^{-1} for the NF strain, and similarly, with the exception of a_x = 43 nM h^{-1} and k = 200 h^{-1}, for the NFpump strain.

Figure 4. Experimentally measured dose-responses of the NR, NRpump and NRpumpmutant strains. (A) Experimentally measured histograms of fluorescence intensity for the NRpump-312 strain, indicating Pdr5p-312::GFP expression at increasing doxycycline concentrations. **(B)** Experimentally measured histograms of fluorescence intensity for the NRpump-558 strain, indicating Pdr5p-558::GFP expression at increasing doxycycline concentrations. **(C)** Experimentally measured dose-responses of NR

(black), NRpump (red) and NRpumpmutant (green, blue) fluorescence means indicate that eliminating the pump function is insufficient to recover the NR dose-response. **(D)** Experimentally measured dose-responses of NR (black), NRpump (red) and NRpumpmutant (green, blue) fluorescence CVs.

Figure 5. Experimentally measured dose-responses of the NF, NFpump and NFpumpmutant strains. (A) Experimentally measured histograms of fluorescence intensity for the NFpump-312 strain, indicating Pdr5p-312::GFP expression at increasing doxycycline concentrations. **(B)** Experimentally measured histograms of fluorescence intensity for the NFpump-558 strain, indicating Pdr5p-558::GFP expression at increasing doxycycline concentrations. **(C)** Experimentally measured dose-responses of NF (black), NFpump (red) and NFpumpmutant (green, blue) fluorescence means indicate that eliminating the pump function is insufficient to recover the NF dose-response. **(D)** Experimentally measured dose-responses of NF (black), NFpump (red) and NFpumpmutant (green, blue) fluorescence CVs.

Figure 6. Stochastic simulation of dose-response change in pumpmutant and non-mutant pump strains. (A) Simulated dose-responses of NR (black), NRpump (red), and NRpumpmutant (green, blue) fluorescence means. **(B)** Simulated dose-responses of NR (black), NRpump (red), and NRpumpmutant (green, blue) CVs. **(C)** Simulated dose-responses of NF (black), NFpump (red), and NFpumpmutant (green, blue) fluorescence means. **(D)** Simulated dose-responses of NF (black), NFpump (red), and NFpumpmutant (green, blue) CVs. Parameters were set to: $a_x = a_z = 50$ nM h^{-1}, $l_z = 10$ nM h^{-1}, $b = 10$ nM^{-1}, $C = 10$ [dox] h^{-1}, $d_x = d_z = 0.12$ h^{-1}, $d_y = 1.2$ h^{-1}, $K = 50$ nM, $h = 3.5$, $\theta = 0.44$ nM, $n = 4$, $k = 0$ h^{-1} for NR and NF strains, $a_x = 43$ nM h^{-1} and $k = 200$ h^{-1} for NRpump and NFpump strains, and similarly, with the exception of $a_x = 43$ nM h^{-1} and $k = 10$ h^{-1}, for NRpumpmutant and NFpumpmutant strains.

Figure 7. Regulation schemes for the 2-color (2c) gene circuits. These strains are identical to the corresponding single-color versions (NR, NRpump, NRpumpmutant, NF, NFpump, NFpumpmutant), except for the regulator gene, which is a bifunctional *tetR::mCherry* fusion for two-color strains. Design

schemes for **(A)** ^{2c}NR; **(B)** ^{2c}NRpump; **(C)** ^{2c}NF; **(D)** ^{2c}NFpump; **(E)** ^{2c}NRpump-312; **(F)** ^{2c}NRpump-558; **(G)** ^{2c}NFpump-312; and **(H)** ^{2c}NFpump-558.

Figure 8. Experimentally measured TetR::mCherry expression levels in the NR and NF clones is higher than in other clones. (A) Experimentally measured mean TetR::mCherry and yEGFP::ZeoR fluorescence intensity dose-responses in the NF strain. **(B)** Experimentally measured mean TetR::mCherry and PDR5::GFP fluorescence intensity dose-responses in the NFpump strain. **(C)** Experimentally measured TetR::mCherry fluorescence means of NR, NRpump and NRpumpmutant strains for individual clones. These data indicate that repressor expression is consistently lower in "pump" strains, as predicted computationally. **(D)** Experimentally measured mean TetR::mCherry fluorescence intensities of NF, NFpump and NFpumpmutant strains for individual clones. These data indicate that repressor expression is consistently lower in "pump" strains, as predicted computationally. **(E)** Experimentally measured dose-responses of mean NR, NRpump and NRpumpmutant TetR::mCherry fluorescence intensities. **(F)** Experimentally measured dose-responses of mean NF, NFpump and NFpumpmutant TetR::mCherry fluorescence intensities. Data shown in panels (E) and (F) was an average of 3 replicates, indicating that repressor expression was higher in NR and NF clones than in any other clones at all doxycycline doses.

SUPPORTING INFORMATION

SUPPORTING FIGURES

Figure S1. Dose-responses of mean fluorescence intensity for NR cells with the native copy of *PDR5* present at its endogenous locus (black) versus NR cells with endogenous *PDR5* knocked out (magenta). Dose-responses of mean fluorescence intensity (calculated using an average of 3 replicates) indicate that the presence/absence of PDR5 at its native locus does not affect the dose-response.

Figure S2. Fitting the NR model to the experimental data. NR ODE, NR analytic, and NR experimental mean dose-responses. The parameters for NR ODE and NR analytic were obtained partly from an earlier study and partly by using Matlab's curve fitting toolbox (see the Methods and the legend of Fig. 2): $a_x = a_z = 9.418$ nM h^{-1}, $l_z = 0.1$ nM h^{-1}, $b = 7.7877$ nM^{-1} h^{-1}, $C = 1.837$ [dox] h^{-1}, $d = 0.1313$ h^{-1}, $f = 1.551$ h^{-1}, $n = 2$, $\theta = 1.858$ nM, and $k = 0$ h^{-1}.

Figure S3. Dose-responses of NF fluorescence intensity mean after including the pump term, but without altering TetR synthesis rate. This plot shows that the pump term alone (red) is insufficient to capture all aspects of the NF dose-response change (parameters for NF are as in Figure S2 except $K = 100$ nM, h = 2, and $k = 200$ h^{-1}).

Figure S4. Dose-responses of fluorescence intensity mean without normalization. (A) NR series: NR (black), NRpump (red), NRpumpmutant (green and blue); **(B)** NF series (colors: as for the NR series).

Figure S5 Single-color and 2-color NF fluorescence mean dose-responses. Dose-responses of mean fluorescence intensity (calculated using an average of 3 replicates) indicate linearity up to saturation. The different slopes are most likely due to fusing mCherry to TetR, which can alter synthesis and degradation rates, as well as protein function.

Figure S6. Dose-responses of exponential growth rates. (A) Cells grow exponentially over 12 hours. Natural logarithms of cell densities (circles) are shown for NR (blue) and NRpump (cyan) strains. The

dashed lines are linear fits to the experimental data with slopes of 0.26129, and 0.30217, respectively. **(B)** Exponential growth rates at increasing doxycycline concentrations are shown for NR (blue), NRpump (cyan), NF(red) and NFpump (magenta) strains.

SUPPORTING TABLE

Table S1. Parameter sensitivity analysis for the NRpump model. The quality of the fits was measured using the L1-norm calculated from the difference between simulation results and experimental data for the 10 different doxycycline concentrations used in the dose response experiments:

$$Q = \sum_{i=1}^{N} \left| GFP_{simulation} - GFP_{\exp eriment} \right|_i .$$

The L1-norms of GFP mean and GFP CV for the parameter set before reducing the repressor synthesis rate (as in Figure 2A,B) appear in the left and right columns labeled "0", respectively. The L1-norms were then computed for each parameter in the model by independently varying them up or down twofold. An increase of two-times the parameter value from the main text appears in the column "+", and a decrease by half appears in the column "-". The best fits for GFP mean and GFP CV (lowest L1-norms) are shown in bold in each row. Most parameter changes that improved the fit of the GFP mean decreased the fit quality for the GFP CV and vice versa. The parameter changes that improved the fit (lower L1-norm compared to the "0" column) for both GFP mean and GFP CV are highlighted in yellow, and the overall best fit (a_x, -) is highlighted in green. Note that increasing parameter C (inducer influx rate multiplier) is equivalent to decreasing TetR synthesis rate (since intracellular inducer inactivates TetR).

References

[1] Stephanopoulos, G. (2012) Synthetic biology and metabolic engineering, *ACS Synth Biol 1*, 514-525.

[2] Nielsen, J., Fussenegger, M., Keasling, J., Lee, S. Y., Liao, J. C., Prather, K., and Palsson, B. (2014) Engineering synergy in biotechnology, *Nat Chem Biol 10*, 319-322.

[3] Khalil, A. S., and Collins, J. J. (2010) Synthetic biology: applications come of age, *Nat Rev Genet 11*, 367-379.

[4] Way, J. C., Collins, J. J., Keasling, J. D., and Silver, P. A. (2014) Integrating biological redesign: where synthetic biology came from and where it needs to go, *Cell 157*, 151-161.

[5] Purnick, P. E., and Weiss, R. (2009) The second wave of synthetic biology: from modules to systems, *Nat Rev Mol Cell Biol 10*, 410-422.

[6] Brophy, J. A., and Voigt, C. A. (2014) Principles of genetic circuit design, *Nat Methods 11*, 508-520.

[7] Slusarczyk, A. L., Lin, A., and Weiss, R. (2012) Foundations for the design and implementation of synthetic genetic circuits, *Nat Rev Genet 13*, 406-420.

[8] Gardner, T. S., Cantor, C. R., and Collins, J. J. (2000) Construction of a genetic toggle switch in Escherichia coli, *Nature 403*, 339-342.

[9] Tigges, M., Marquez-Lago, T. T., Stelling, J., and Fussenegger, M. (2009) A tunable synthetic mammalian oscillator, *Nature 457*, 309-312.

[10] Siuti, P., Yazbek, J., and Lu, T. K. (2013) Synthetic circuits integrating logic and memory in living cells, *Nat Biotechnol 31*, 448-452.

[11] Xie, Z., Wroblewska, L., Prochazka, L., Weiss, R., and Benenson, Y. (2011) Multi-input RNAi-based logic circuit for identification of specific cancer cells, *Science 333*, 1307-1311.

[12] Moon, T. S., Lou, C., Tamsir, A., Stanton, B. C., and Voigt, C. A. (2012) Genetic programs constructed from layered logic gates in single cells, *Nature 491*, 249-253.

[13] Nandagopal, N., and Elowitz, M. B. (2011) Synthetic biology: integrated gene circuits, *Science 333*, 1244-1248.

[14] Stricker, J., Cookson, S., Bennett, M. R., Mather, W. H., Tsimring, L. S., and Hasty, J. (2008) A fast, robust and tunable synthetic gene oscillator, *Nature 456*, 516-519.

[15] Elowitz, M. B., and Leibler, S. (2000) A synthetic oscillatory network of transcriptional regulators, *Nature 403*, 335-338.

[16] Nevozhay, D., Adams, R. M., Murphy, K. F., Josic, K., and Balazsi, G. (2009) Negative autoregulation linearizes the dose-response and suppresses the heterogeneity of gene expression, *Proc Natl Acad Sci U S A 106*, 5123-5128.

[17] Ellis, T., Wang, X., and Collins, J. J. (2009) Diversity-based, model-guided construction of synthetic gene networks with predicted functions, *Nat Biotechnol 27*, 465-471.

[18] Nissim, L., Perli, S. D., Fridkin, A., Perez-Pinera, P., and Lu, T. K. (2014) Multiplexed and programmable regulation of gene networks with an integrated RNA and CRISPR/Cas toolkit in human cells, *Mol Cell 54*, 698-710.

[19] Nevozhay, D., Zal, T., and Balazsi, G. (2013) Transferring a synthetic gene circuit from yeast to mammalian cells, *Nat Commun 4*, 1451.

[20] Bleris, L., Xie, Z., Glass, D., Adadey, A., Sontag, E., and Benenson, Y. (2011) Synthetic incoherent feedforward circuits show adaptation to the amount of their genetic template, *Mol Syst Biol 7*, 519.

[21] Dunlop, M. J., Dossani, Z. Y., Szmidt, H. L., Chu, H. C., Lee, T. S., Keasling, J. D., Hadi, M. Z., and Mukhopadhyay, A. (2011) Engineering microbial biofuel tolerance and export using efflux pumps, *Mol Syst Biol 7*, 487.

[22] Harrison, M. E., and Dunlop, M. J. (2012) Synthetic feedback loop model for increasing microbial biofuel production using a biosensor, *Front Microbiol 3*, 360.
[23] Lage, H. (2003) ABC-transporters: implications on drug resistance from microorganisms to human cancers, *Int J Antimicrob Agents 22*, 188-199.
[24] Charlebois, D. A., Balazsi, G., and Kaern, M. (2014) Coherent feedforward transcriptional regulatory motifs enhance drug resistance, *Physical Review E 89*.
[25] Sauna, Z. E., Bohn, S. S., Rutledge, R., Dougherty, M. P., Cronin, S., May, L., Xia, D., Ambudkar, S. V., and Golin, J. (2008) Mutations define cross-talk between the N-terminal nucleotide-binding domain and transmembrane helix-2 of the yeast multidrug transporter Pdr5: possible conservation of a signaling interface for coupling ATP hydrolysis to drug transport, *J Biol Chem 283*, 35010-35022.
[26] Ananthaswamy, N., Rutledge, R., Sauna, Z. E., Ambudkar, S. V., Dine, E., Nelson, E., Xia, D., and Golin, J. (2010) The signaling interface of the yeast multidrug transporter Pdr5 adopts a cis conformation, and there are functional overlap and equivalence of the deviant and canonical Q-loop residues, *Biochemistry 49*, 4440-4449.
[27] Ino, K., Kitagawa, Y., Watanabe, T., Shiku, H., Koide, M., Itayama, T., Yasukawa, T., and Matsue, T. (2009) Detection of hormone active chemicals using genetically engineered yeast cells and microfluidic devices with interdigitated array electrodes, *Electrophoresis 30*, 3406-3412.
[28] Murphy, K. F., Balazsi, G., and Collins, J. J. (2007) Combinatorial promoter design for engineering noisy gene expression, *Proc Natl Acad Sci U S A 104*, 12726-12731.
[29] Rogers, B., Decottignies, A., Kolaczkowski, M., Carvajal, E., Balzi, E., and Goffeau, A. (2001) The pleitropic drug ABC transporters from Saccharomyces cerevisiae, *J Mol Microbiol Biotechnol 3*, 207-214.
[30] Kolaczkowski, M., van der Rest, M., Cybularz-Kolaczkowska, A., Soumillion, J. P., Konings, W. N., and Goffeau, A. (1996) Anticancer drugs, ionophoric peptides, and steroids as substrates of the yeast multidrug transporter Pdr5p, *J Biol Chem 271*, 31543-31548.
[31] Kolaczkowski, M., Kolaczowska, A., Luczynski, J., Witek, S., and Goffeau, A. (1998) In vivo characterization of the drug resistance profile of the major ABC transporters and other components of the yeast pleiotropic drug resistance network, *Microb Drug Resist 4*, 143-158.
[32] Newman, J. R., Ghaemmaghami, S., Ihmels, J., Breslow, D. K., Noble, M., DeRisi, J. L., and Weissman, J. S. (2006) Single-cell proteomic analysis of S. cerevisiae reveals the architecture of biological noise, *Nature 441*, 840-846.
[33] Lu, P., Vogel, C., Wang, R., Yao, X., and Marcotte, E. M. (2007) Absolute protein expression profiling estimates the relative contributions of transcriptional and translational regulation, *Nat Biotechnol 25*, 117-124.
[34] Dublanche, Y., Michalodimitrakis, K., Kummerer, N., Foglierini, M., and Serrano, L. (2006) Noise in transcription negative feedback loops: simulation and experimental analysis, *Mol Syst Biol 2*, 41.
[35] Simpson, M. L., Cox, C. D., and Sayler, G. S. (2003) Frequency domain analysis of noise in autoregulated gene circuits, *Proc Natl Acad Sci U S A 100*, 4551-4556.
[36] Becskei, A., and Serrano, L. (2000) Engineering stability in gene networks by autoregulation, *Nature 405*, 590-593.
[37] Murphy, K. F., Adams, R. M., Wang, X., Balazsi, G., and Collins, J. J. (2010) Tuning and controlling gene expression noise in synthetic gene networks, *Nucleic Acids Res 38*, 2712-2726.
[38] Klumpp, S., and Hwa, T. (2014) Bacterial growth: global effects on gene expression, growth feedback and proteome partition, *Curr Opin Biotechnol 28*, 96-102.
[39] Tan, C., Marguet, P., and You, L. (2009) Emergent bistability by a growth-modulating positive feedback circuit, *Nat Chem Biol 5*, 842-848.

[40] Airoldi, E. M., Huttenhower, C., Gresham, D., Lu, C., Caudy, A. A., Dunham, M. J., Broach, J. R., Botstein, D., and Troyanskaya, O. G. (2009) Predicting cellular growth from gene expression signatures, *PLoS Comput Biol 5*, e1000257.

[41] Klumpp, S., Zhang, Z., and Hwa, T. (2009) Growth rate-dependent global effects on gene expression in bacteria, *Cell 139*, 1366-1375.

[42] Levy, S., and Barkai, N. (2009) Coordination of gene expression with growth rate: a feedback or a feed-forward strategy?, *FEBS Lett 583*, 3974-3978.

[43] Garcia-Bernardo, J., and Dunlop, M. J. (2013) Tunable stochastic pulsing in the Escherichia coli multiple antibiotic resistance network from interlinked positive and negative feedback loops, *PLoS Comput Biol 9*, e1003229.

[44] Boyarskiy, S., Lopez, S. D., Kong, N. W., and Tullman-Ercek, D. (2016) Transcriptional feedback regulation of efflux protein expression for increased tolerance to and production of n-butanol, *Metabolic Engineering 33*, 130-137.

[45] Eldakak, A., Rancati, G., Rubinstein, B., Paul, P., Conaway, V., and Li, R. (2010) Asymmetrically inherited multidrug resistance transporters are recessive determinants in cellular replicative ageing, *Nat Cell Biol 12*, 799-805.

[46] Blake, W. J., Balazsi, G., Kohanski, M. A., Isaacs, F. J., Murphy, K. F., Kuang, Y., Cantor, C. R., Walt, D. R., and Collins, J. J. (2006) Phenotypic consequences of promoter-mediated transcriptional noise, *Mol Cell 24*, 853-865.

[47] Ozbudak, E. M., Thattai, M., Kurtser, I., Grossman, A. D., and van Oudenaarden, A. (2002) Regulation of noise in the expression of a single gene, *Nat Genet 31*, 69-73.

[48] Elowitz, M. B., Levine, A. J., Siggia, E. D., and Swain, P. S. (2002) Stochastic gene expression in a single cell, *Science 297*, 1183-1186.

[49] Blake, W. J., M, K. A., Cantor, C. R., and Collins, J. J. (2003) Noise in eukaryotic gene expression, *Nature 422*, 633-637.

[50] Fraser, H. B., Hirsh, A. E., Giaever, G., Kumm, J., and Eisen, M. B. (2004) Noise minimization in eukaryotic gene expression, *PLoS Biol 2*, e137.

[51] Huh, W. K., Falvo, J. V., Gerke, L. C., Carroll, A. S., Howson, R. W., Weissman, J. S., and O'Shea, E. K. (2003) Global analysis of protein localization in budding yeast, *Nature 425*, 686-691.

[52] Nevozhay, D., Adams, R. M., and Balazsi, G. (2011) Linearizer Gene Circuits with Negative Feedback Regulation, *Yeast Genetic Networks: Methods and Protocols 734*, 81-100.

[53] Gietz, R. D., Schiestl, R. H., Willems, A. R., and Woods, R. A. (1995) Studies on the transformation of intact yeast cells by the LiAc/SS-DNA/PEG procedure, *Yeast 11*, 355-360.

[54] Gillespie, D. T. (1976) A General Method for Numerically Simulating the Stochastic Time Evolution of Coupled Chemical Reactions, *Journal of Computational Physics 22*, 403–434.

[55] Gillespie, D. T. (1977) Exact Stochastic Simulation of Coupled Chemical-Reactions, *Journal of Physical Chemistry 81*, 2340-2361.

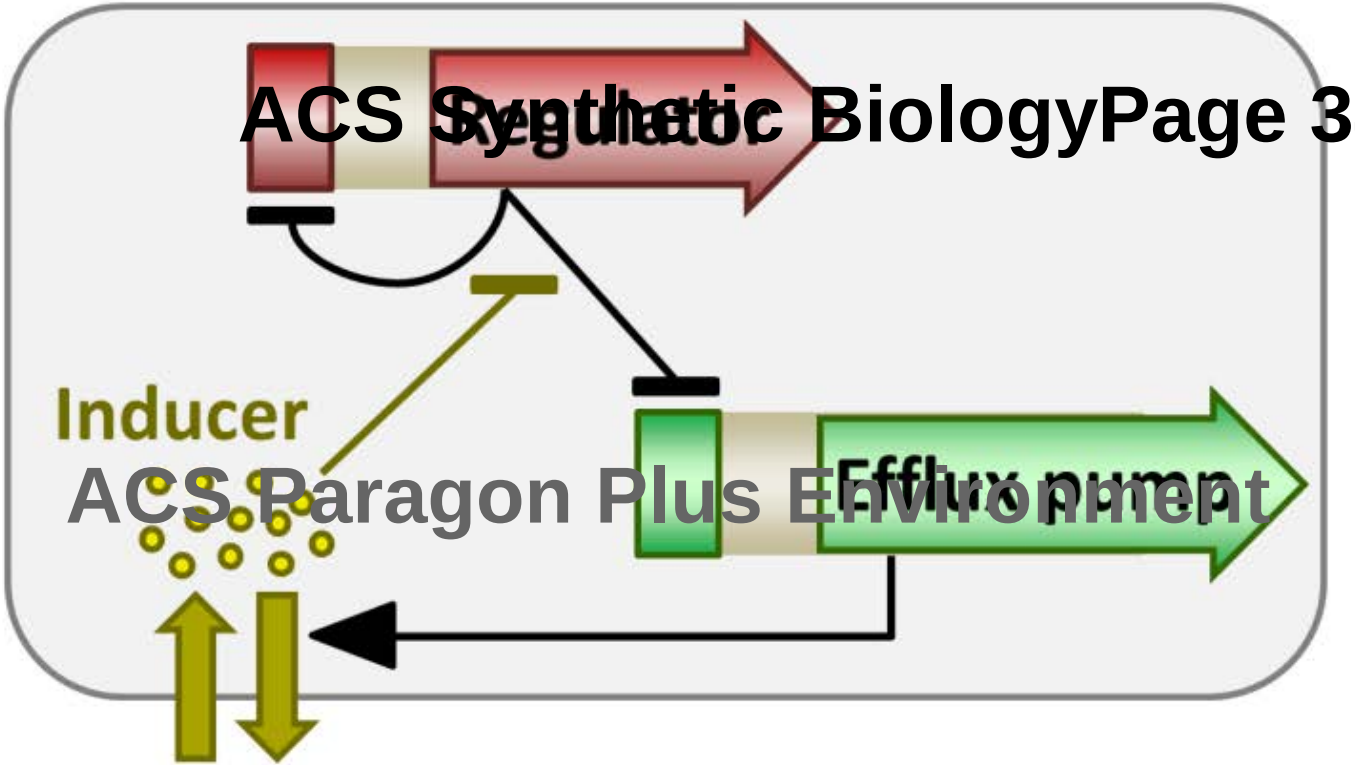

Figure 1

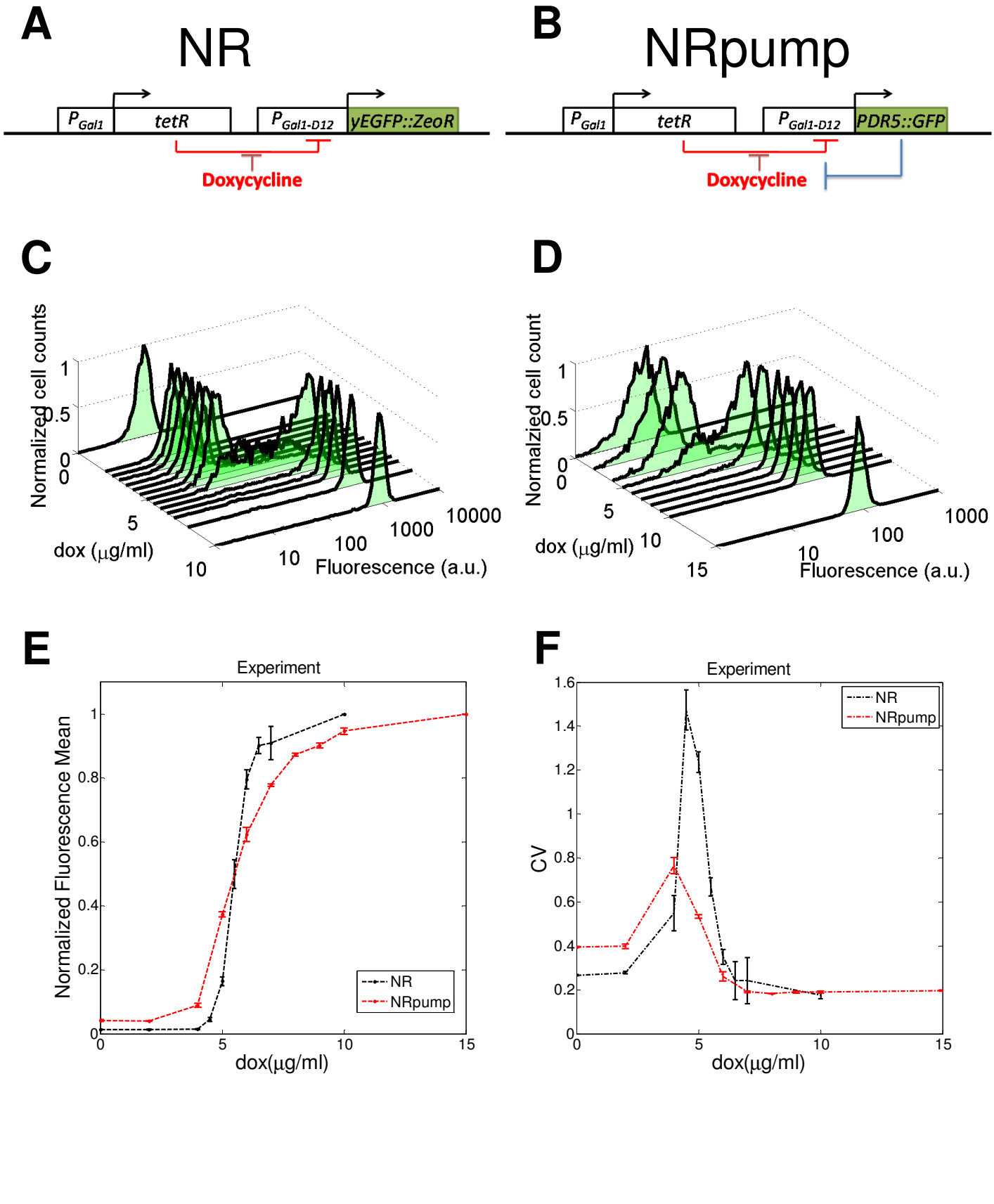
A
NR
P Gal1
tetR
P Gal1-D12
yEGFP::ZeoR
Doxycycline
B
NRpump
P Gal1
tetR
P Gal1-D12
PDR5::GFP
Doxycycline
C
Normalized cell counts
dox (μg/ml)
Fluorescence (a.u.)
D
Normalzied cell count
dox (μg/ml)
Fluorescence (a.u.)
E
Experiment
Normalized Fluorescence Mean
dox(μg/ml)
NR
NRpump
F
Experiment
CV
dox(μg/ml)
NR
NRpump

Figure 2

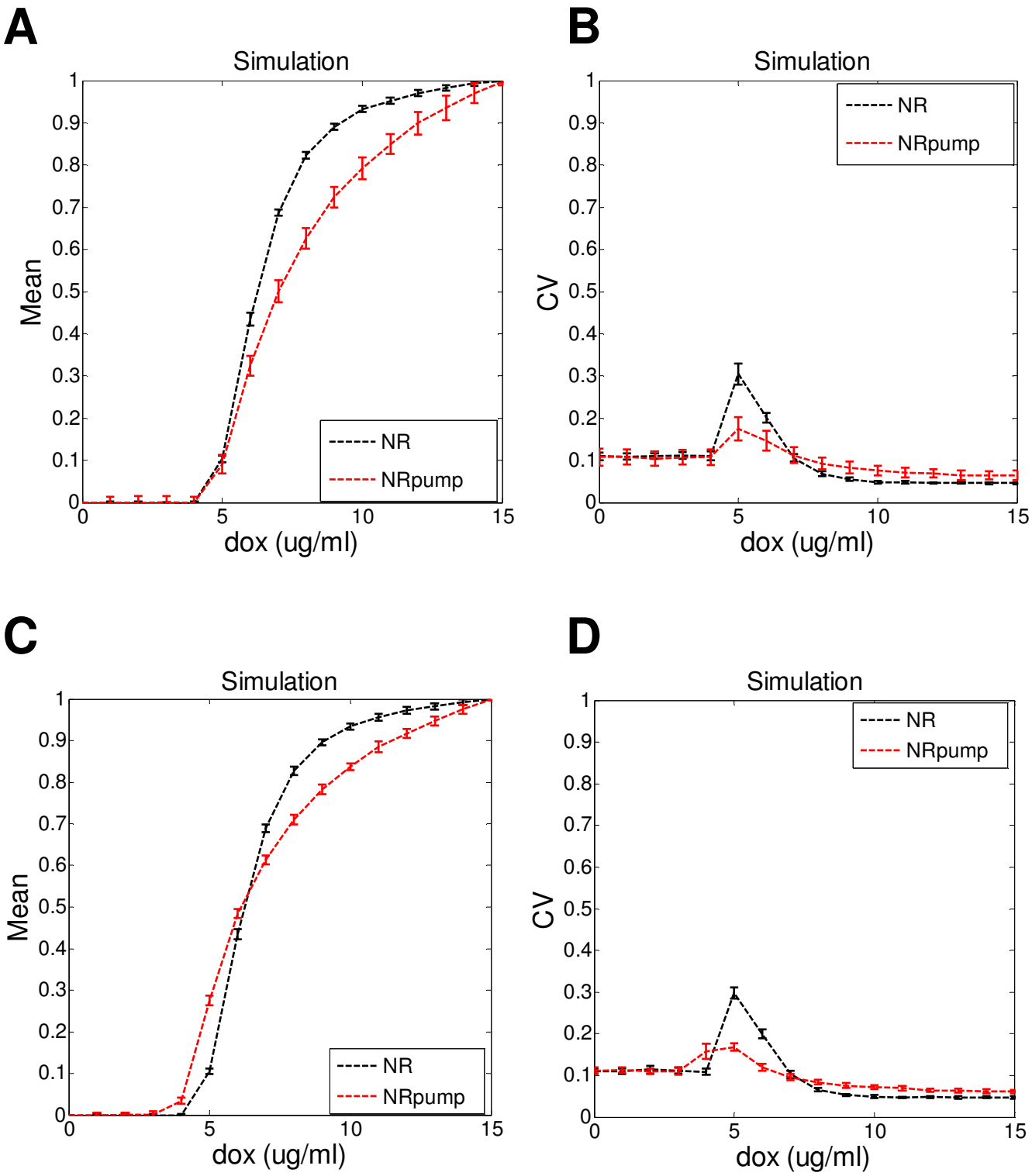
A
Simulation
Mean
dox (ug/ml)
NR
NRpump
B
Simulation
CV
dox (ug/ml)
NR
NRpump
C
Simulation
Mean
dox (ug/ml)
NR
NRpump
D
Simulation
CV
dox (ug/ml)
NR
NRpump

Figure 3

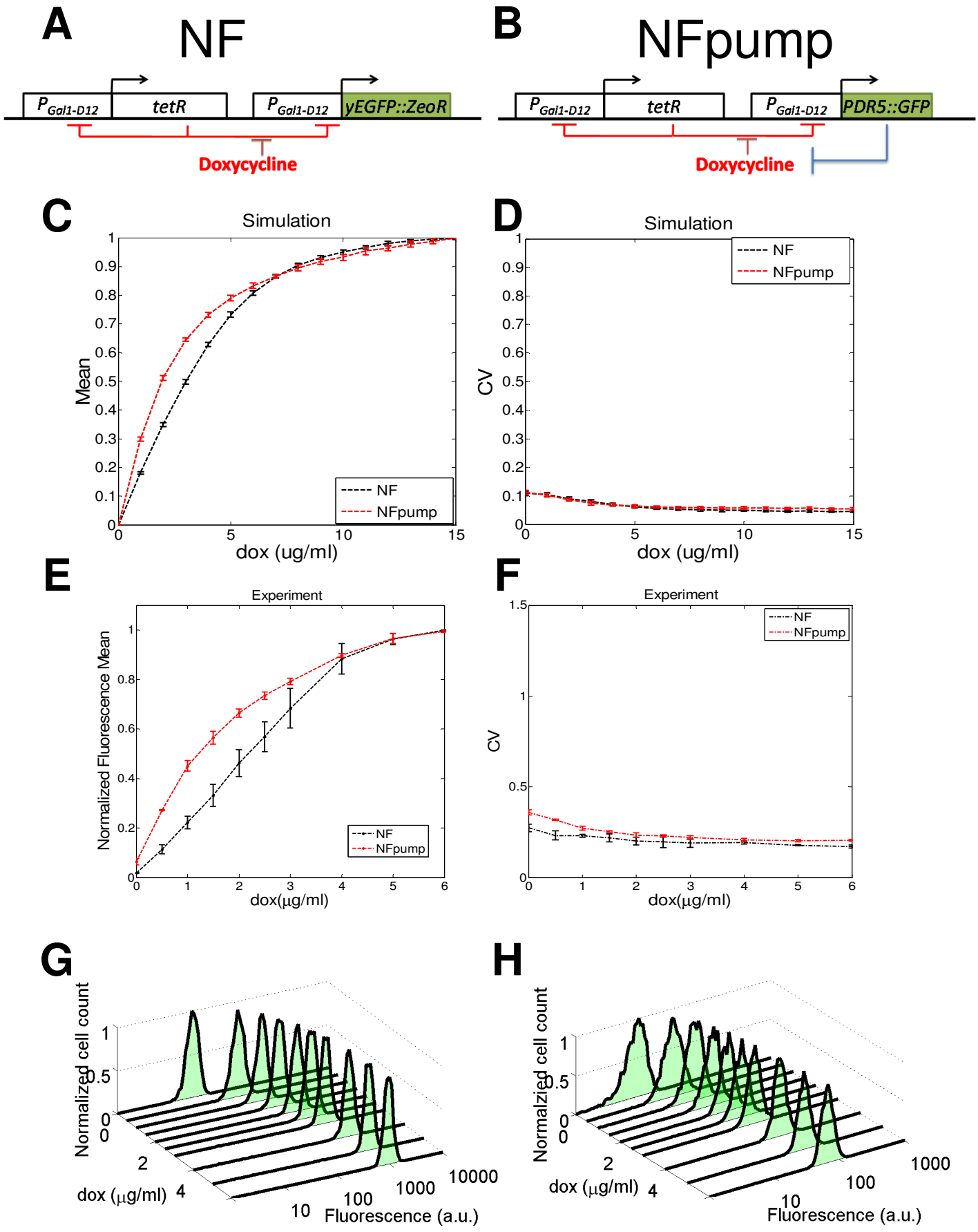
A
NF
$P_{Gal1-D12}$
tetR
$P_{Gal1-D12}$
yEGFP::ZeoR
Doxycycline
B
NFpump
$P_{Gal1-D12}$
tetR
$P_{Gal1-D12}$
PDR5::GFP
Doxycycline
C
Simulation
Mean
dox (ug/ml)
NF
NFpump
D
Simulation
CV
dox (ug/ml)
NF
NFpump
E
Experiment
Normalized Fluorescence Mean
dox(μg/ml)
NF
NFpump
F
Experiment
CV
dox(μg/ml)
NF
NFpump
G
Normalized cell count
dox (μg/ml)
Fluorescence (a.u.)
H
Normalized cell count
dox (μg/ml)
Fluorescence (a.u.)

Figure 4

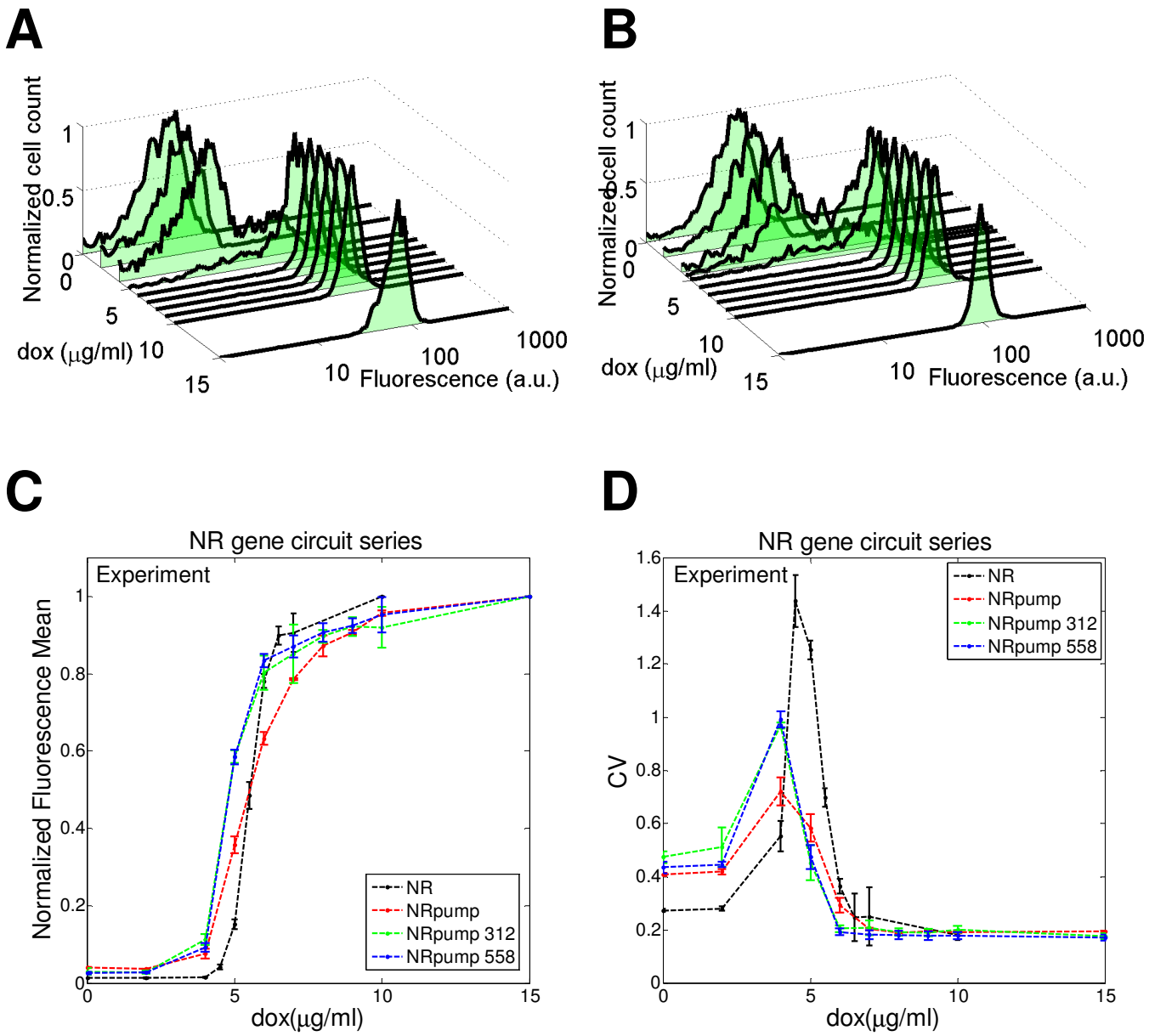
A
Normalized cell count
1
0.5
0
0
5
dox (μg/ml) 10
15
10
100
1000
Fluorescence (a.u.)
B
Normalized cell count
1
0.5
0
0
5
10
dox (μg/ml)
15
10
100
1000
Fluorescence (a.u.)
C
NR gene circuit series
Experiment
Normalized Fluorescence Mean
dox(μg/ml)
NR
NRpump
NRpump 312
NRpump 558
D
NR gene circuit series
Experiment
CV
dox(μg/ml)
NR
NRpump
NRpump 312
NRpump 558

Figure 5

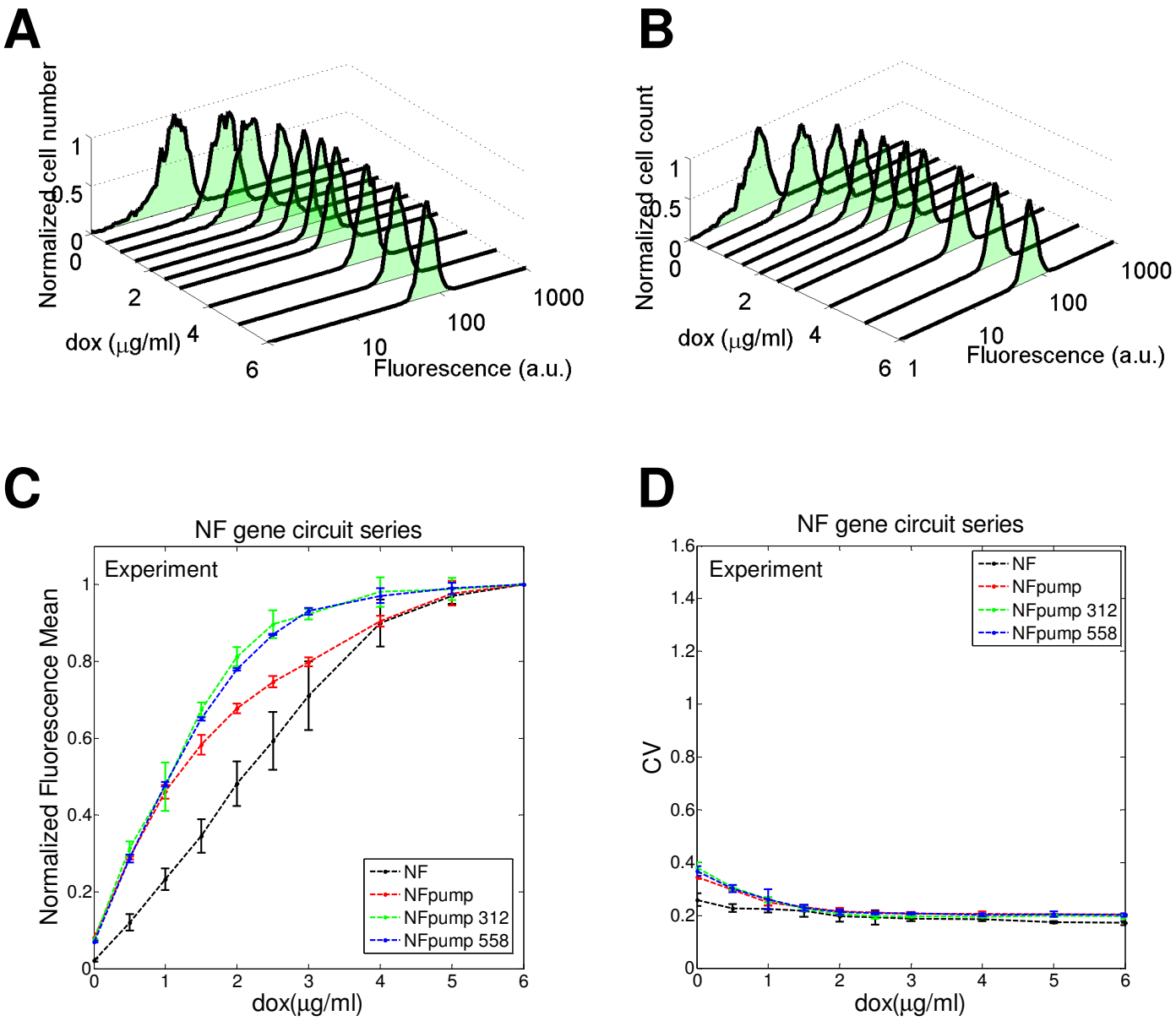
A
Normalized cell number
dox (μg/ml)
Fluorescence (a.u.)
B
Normalized cell count
dox (μg/ml)
Fluorescence (a.u.)
C
NF gene circuit series
Experiment
Normalized Fluorescence Mean
dox(μg/ml)
NF
NFpump
NFpump 312
NFpump 558
D
NF gene circuit series
Experiment
CV
dox(μg/ml)
NF
NFpump
NFpump 312
NFpump 558

Figure 6

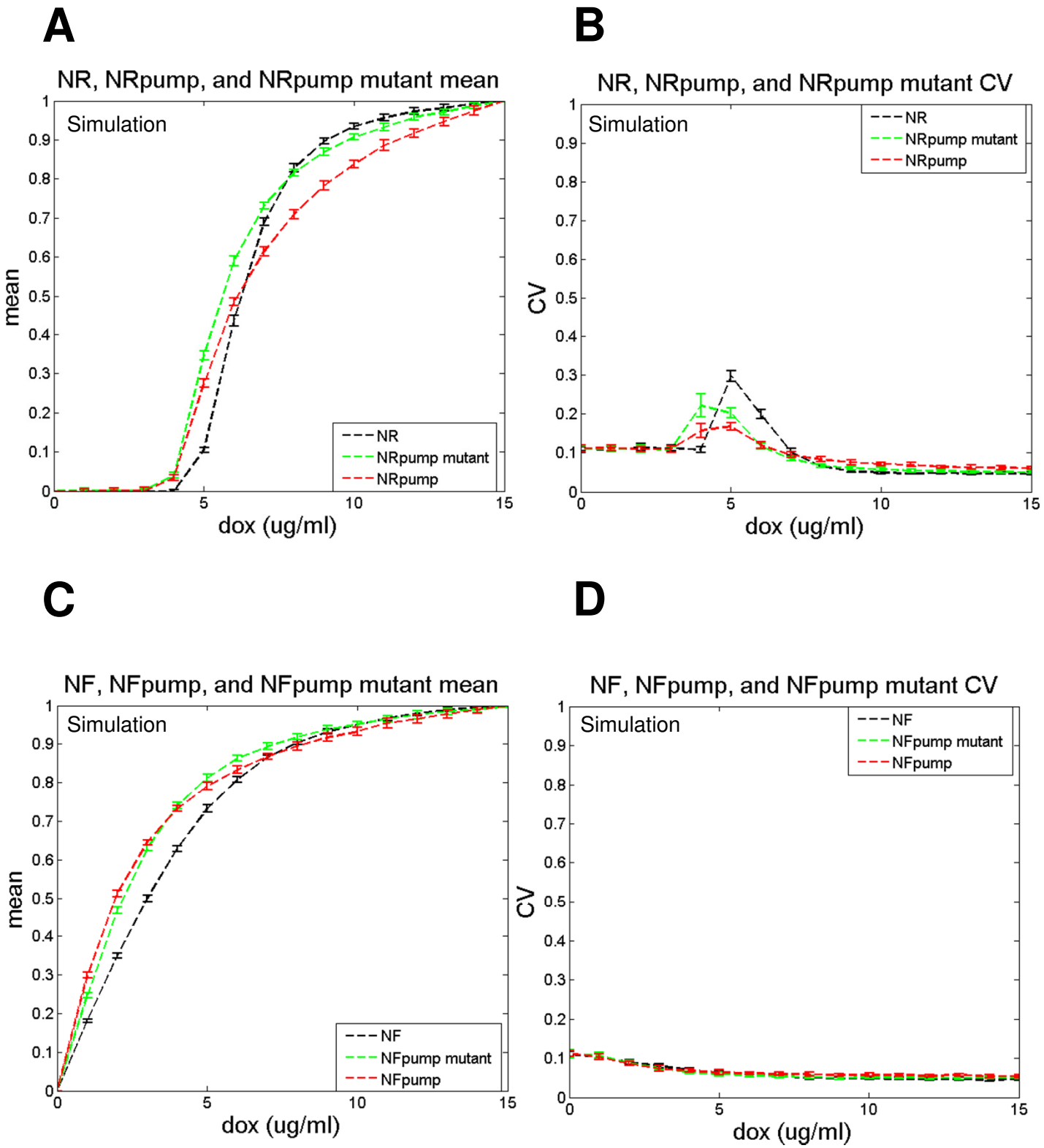
A
NR, NRpump, and NRpump mutant mean
Simulation
mean
dox (ug/ml)
NR
NRpump mutant
NRpump
B
NR, NRpump, and NRpump mutant CV
Simulation
CV
dox (ug/ml)
NR
NRpump mutant
NRpump
C
NF, NFpump, and NFpump mutant mean
Simulation
mean
dox (ug/ml)
NF
NFpump mutant
NFpump
D
NF, NFpump, and NFpump mutant CV
Simulation
CV
dox (ug/ml)
NF
NFpump mutant
NFpump

Figure 7

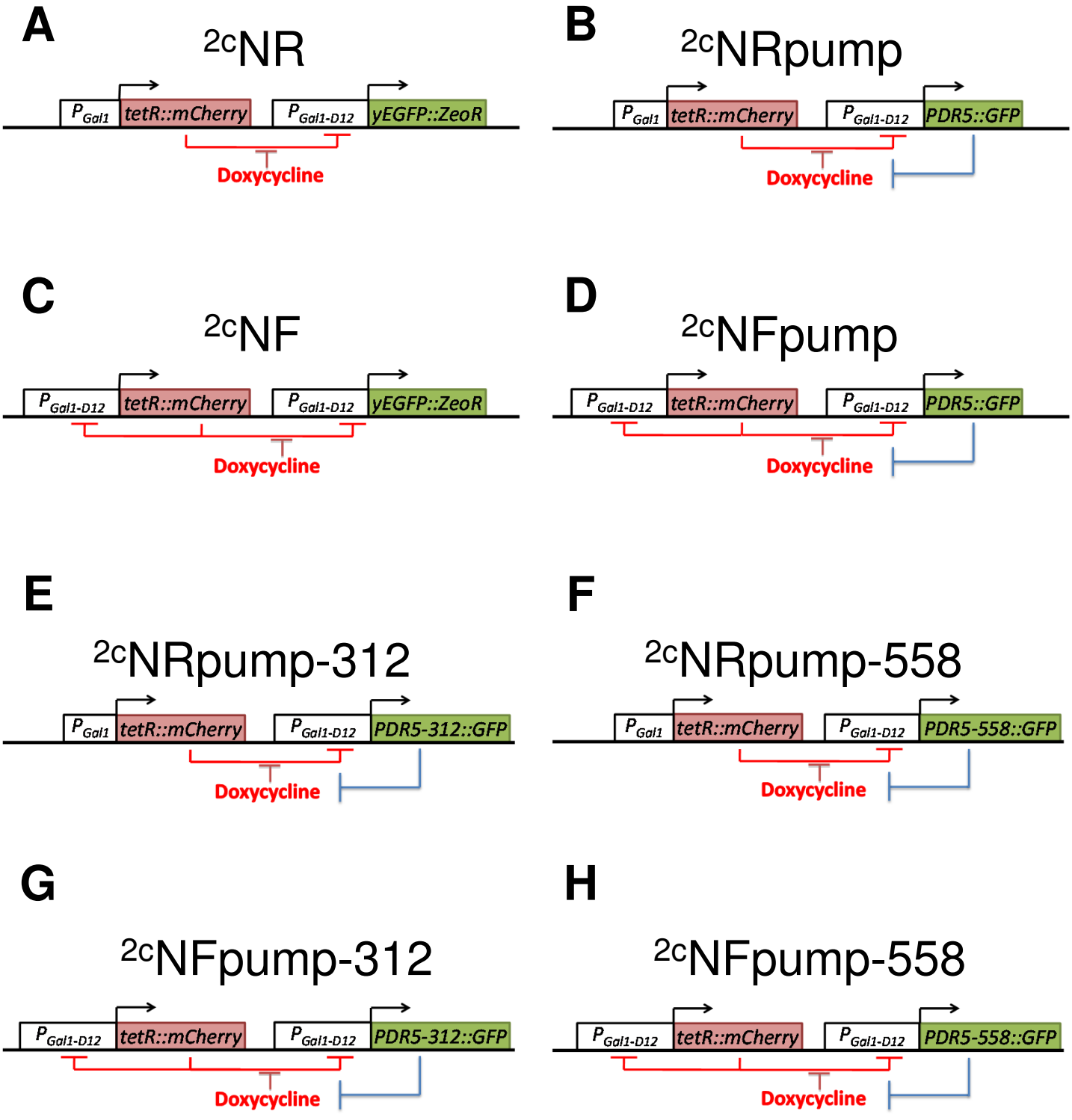
A
2cNR
PGal1
tetR::mCherry
PGal1-D12
yEGFP::ZeoR
Doxycycline
B
2cNRpump
PGal1
tetR::mCherry
PGal1-D12
PDR5::GFP
Doxycycline
C
2cNF
PGal1-D12
tetR::mCherry
PGal1-D12
yEGFP::ZeoR
Doxycycline
D
2cNFpump
PGal1-D12
tetR::mCherry
PGal1-D12
PDR5::GFP
Doxycycline
E
2cNRpump-312
PGal1
tetR::mCherry
PGal1-D12
PDR5-312::GFP
Doxycycline
F
2cNRpump-558
PGal1
tetR::mCherry
PGal1-D12
PDR5-558::GFP
Doxycycline
G
2cNFpump-312
PGal1-D12
tetR::mCherry
PGal1-D12
PDR5-312::GFP
Doxycycline
H
2cNFpump-558
PGal1-D12
tetR::mCherry
PGal1-D12
PDR5-558::GFP
Doxycycline

Figure 8

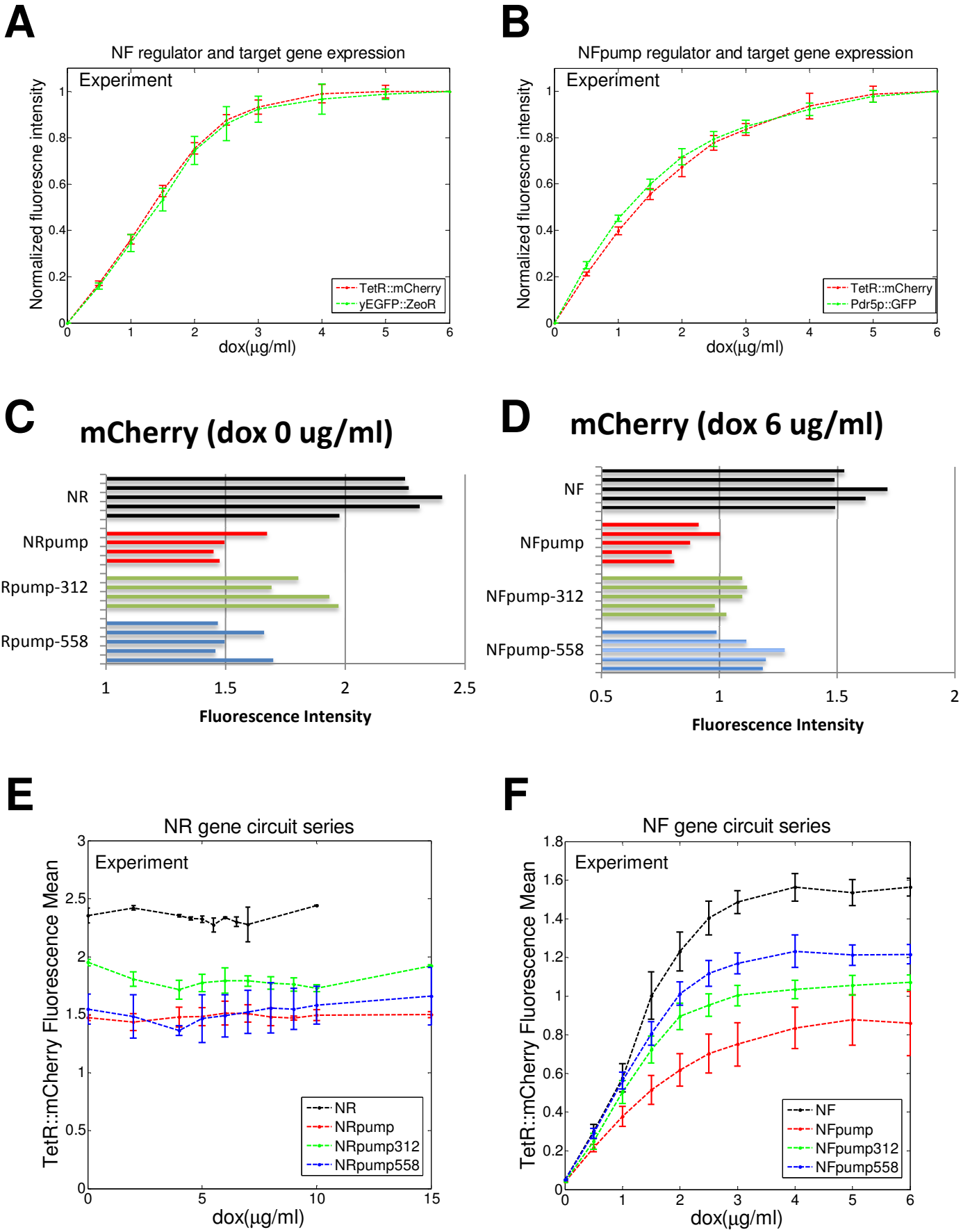
A
NF regulator and target gene expression
Experiment
Normalized fluorescne intensity
dox(μg/ml)
TetR::mCherry
yEGFP::ZeoR
B
NFpump regulator and target gene expression
Experiment
Normalized fluorescne intensity
dox(μg/ml)
TetR::mCherry
Pdr5p::GFP
C
mCherry (dox 0 ug/ml)
NR
NRpump
NRpump-312
NRpump-558
Fluorescence Intensity
D
mCherry (dox 6 ug/ml)
NF
NFpump
NFpump-312
NFpump-558
Fluorescence Intensity
E
NR gene circuit series
Experiment
TetR::mCherry Fluorescence Mean
dox(μg/ml)
NR
NRpump
NRpump312
NRpump558
F
NF gene circuit series
Experiment
TetR::mCherry Fluorescence Mean
dox(μg/ml)
NF
NFpump
NFpump312
NFpump558